ONLINE SUPPLEMENTAL APPENDICES

Supplemental Appendix S1: Additional field results

In this appendix, we provide additional results related to field sampling of epidemics and variation among lakes in seasonal patterns of resource quality. First, we show that in the intensively sampled epidemics, the seasonal egg ratio signature observed for uninfected hosts correlates strongly with that for infected hosts – infected hosts produce fewer eggs overall but still respond to changes in resource quality as do uninfected hosts (Figure S1). Second, we see how per capita birth rate changes through time during epidemics. To calculate birth rate, we used the egg ratio method (Paloheimo 1974) which involves converting egg ratios (Figure 1) into a birth rate using a temperature-dependent development time (Rigler and Downing 1984). To add the thermal dimension, we combined vertical temperature measurements, day-night sampling of the populations (using a 20 L Schindler trap deployed at 1 m intervals), and changes in daylight throughout the season. We show birth rates per capita (juveniles plus adults) and per adult (Figure S2). Birth rates do not mirror the egg ratio (resource quality) signal shown in Figure 1 because temperature declines throughout during autumn counter-balance the increase in egg ratios. Instead, per adult birth rates fluctuate around a fairly constant mean. Without the increase in resource quality, birth rate would decline considerably with dropping temperatures in autumn. However, we do see strong temperature-egg ratio correlations during each epidemic: as temperatures cooled, resource quality increased (Figure S3).


Additional Literature Cited:

Paloheimo, J.E. (1974). Calculation of instantaneous birth rate. *Limnol. Oceanogr.,* 19, 692–694.

Rigler, F. H., and J. A. Downing. (1984). The calculation of secondary productivity, In: A manual on methods for the assessment of secondary productivity in freshwater. (eds.

Downing, J.A. & Rigler, F.H.) International Biological Program Handbook 17.

Blackwell Scientific, pp. 19–58.

Figure S1. Comparison of egg ratios in uninfected and infected hosts (*Daphnia dentifera*)

30   during the course of three epidemics of a virulent fungus (*Metschnikowia bicuspidata*) during

2004. Egg ratios of infected hosts were lower than uninfected hosts, but tended to follow the

same seasonal trajectories.
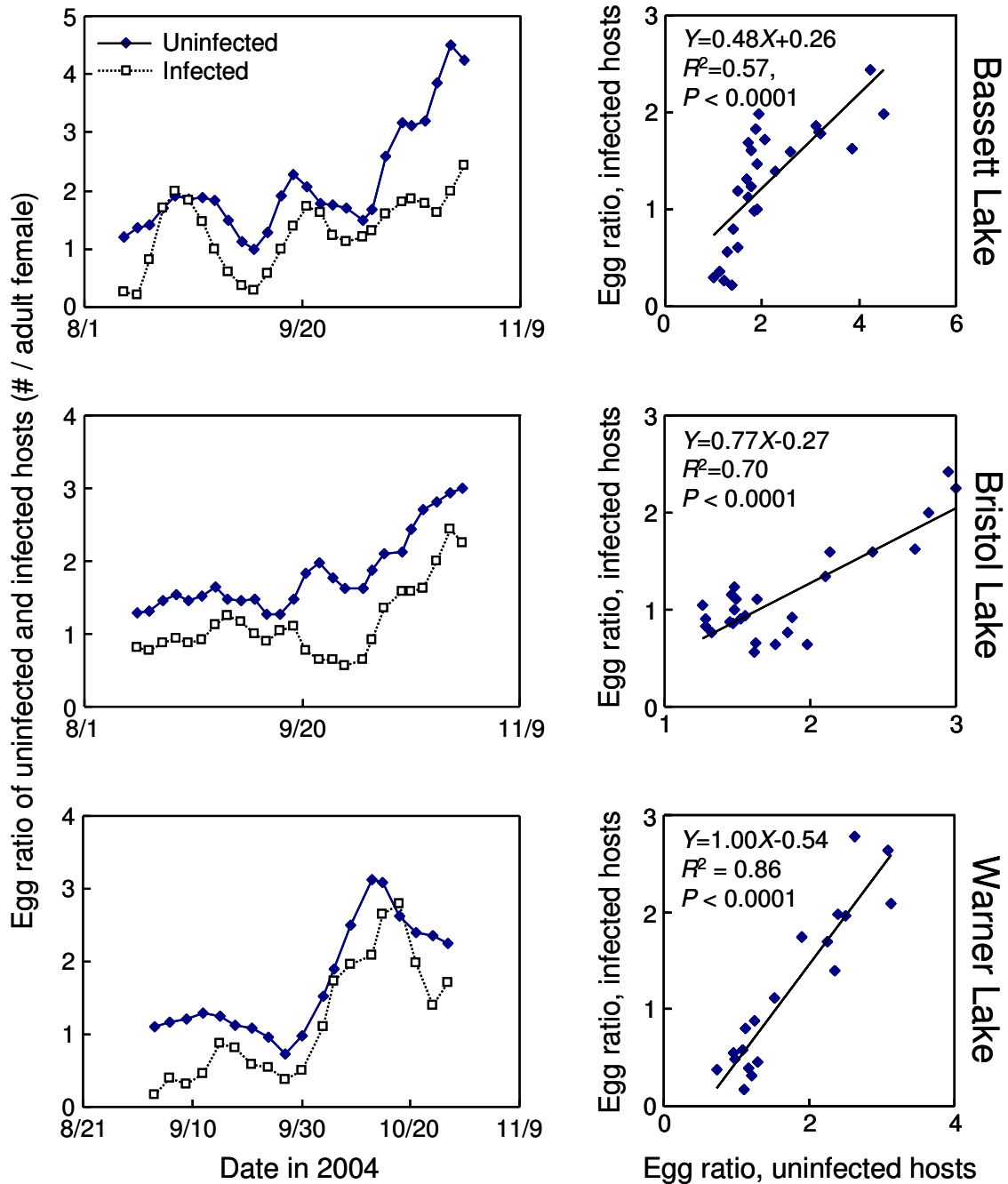
Figure S2. Birth rates of the host *Daphnia dentifera* scaled to (A) per capita (i.e., juveniles + adults) and (B) just adult females in the three intensively sampled lakes during 2004. Also presented is weighted temperature experienced by the migrating host.
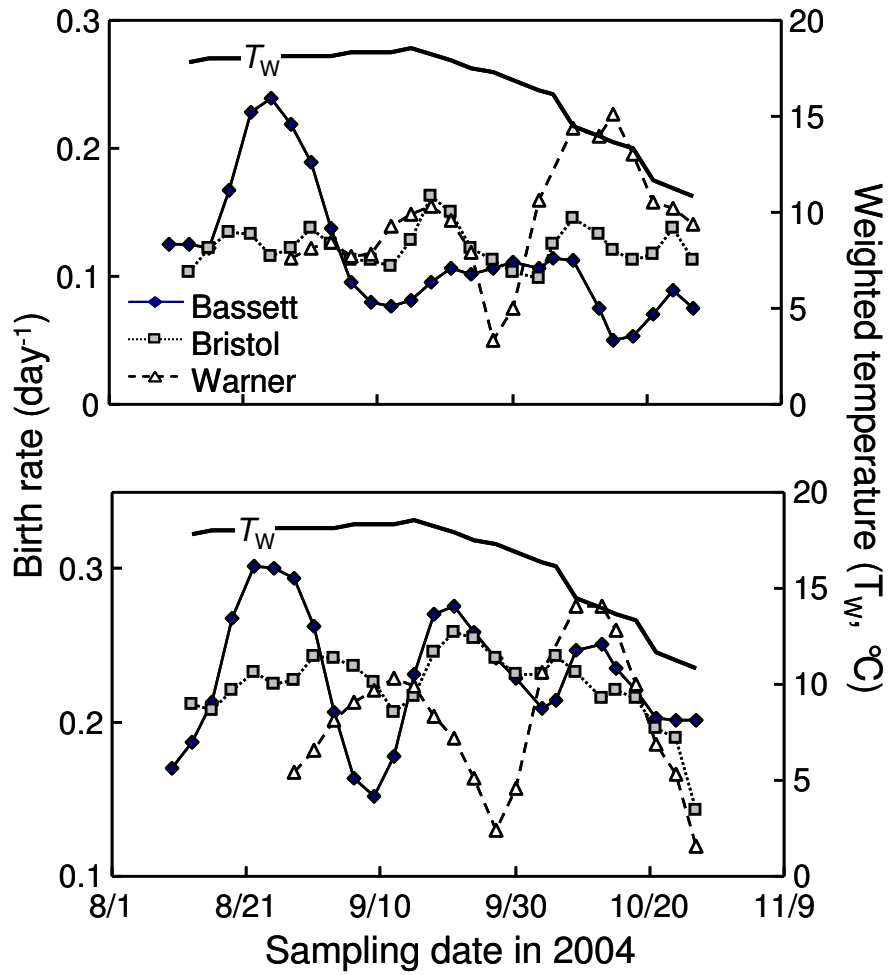
Figure S3. Correlations between weighted temperature and the egg ratio-based index of resource quality from the three intensively sampled epidemics (2004) of the virulent fungus *Metschnikowia bicuspidata* in lake *Daphnia dentifera* populations.

40
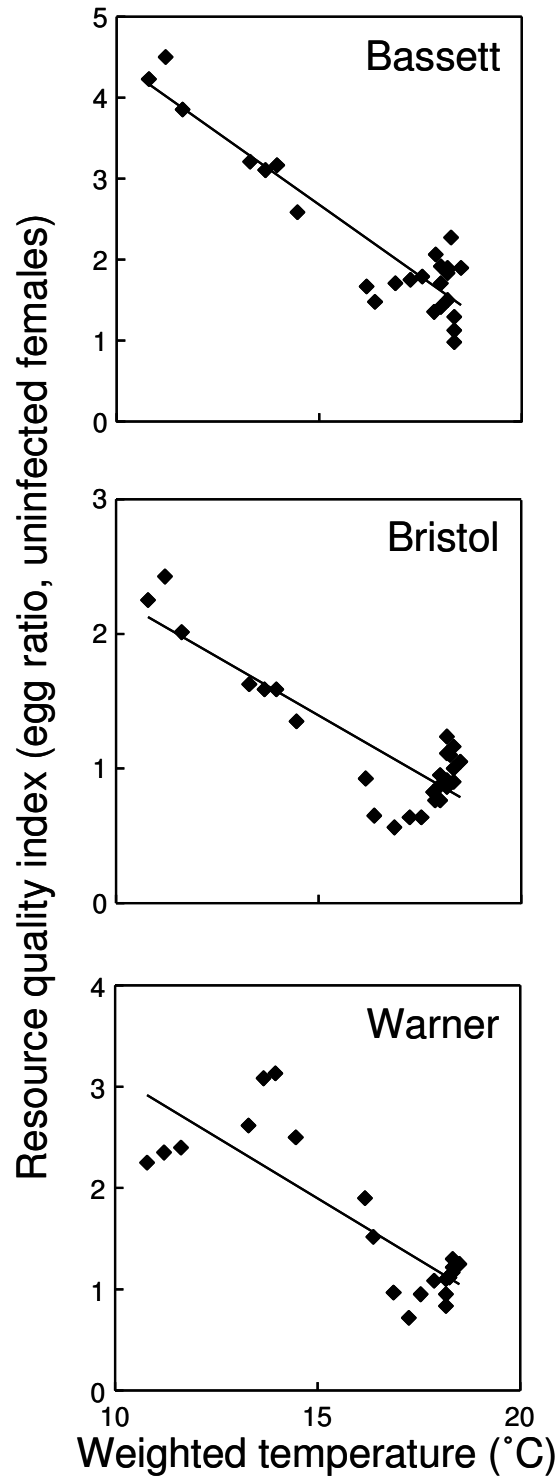
Supplemental Appendix S2: Additional theoretical results

In this Supplemental Appendix, we expand our analysis of the dynamic epidemiological model for susceptible hosts (S), infected hosts (I), and free-living spores (Z). In the first case, we marginally expand our result relating change in reproductive ratio (R_0) with small increases in resource quality of the host (Q). We could imagine that the strength of density dependence (c) and background death rate of susceptible hosts (d) both depends on quality; specifically, both should decrease with quality ($\partial c/\partial Q < 0$ and $\partial d/\partial Q < 0$), since higher resource quality at a given quantity should support more hosts, all else being equal, and better fed hosts could live longer. (Of course, resource quality might be too good – *Daphnia*, like other species, can die more quickly when they consume high quantities of excellent food resources). Given this information, and knowing that R_0 increases when c and d shrink, we could imagine rewriting the $\partial R_0/\partial Q$ equation (equ. 4) to include these factors in component B (after equ. 4):

$$\frac{\partial R_0}{\partial Q} = R_0 \left[\underbrace{\frac{1}{\beta}\frac{\partial \beta}{\partial Q}}_{A} + \underbrace{\frac{1}{\sigma}\frac{\partial \sigma}{\partial Q} - \frac{1}{c}\frac{\partial c}{\partial Q} + \left(\frac{d}{b-d}\right)\left(\frac{1}{b}\frac{\partial b}{\partial Q} - \frac{1}{d}\frac{\partial d}{\partial Q}\right)}_{B} \right] \tag{B1}$$

where still now R_0 can with decrease with enhanced quality via the transmission rate effect ($\partial \beta/\partial Q < 0$; Component A) – but this effect must be large enough to counter-act the effects of quality all of the other key parameters (σ, c, b, d; Component B)

In the second expansion, we add more realism to the epidemiological representation of this system, particularly to the equation for free-living spores (Z). First, we re-consider the infection process (equ. B2.a ,b) by breaking the per capita transmission rate (β) into two presumably independent processes, a rate at which susceptible hosts contact and then remove spores (f) and the infectivity of those spores once contacted (u, i.e., $\beta \equiv uf$). Then, we also model removal of free-living spores by both susceptible (S) and infected (I) host classes. For simplicity here, we assume that both host classes remove spores at the same rate and efficiency. This model then becomes:

$$dS/dt = b(S + \rho I)(1 - c(S + I)) - dS - ufSZ \tag{B2.a}$$

$$dI/dt = ufSZ - (d + v)I \tag{B2.b}$$

$$dZ/dt = \sigma(d + v)I - mZ - f(S + I)Z . \tag{B2.c}$$

The key difference between this model and the version presented in the text (equ. 1) centers on
the spore equation (equ. B2.c): both host classes remove spores. Unfortunately, the expressions
for the interior equilibrium for this model are too complex to present simply here (although we
see that density of susceptible hosts drops with f, density of infected hosts first increase and then
decreases with f, and proportion of hosts infected [$I^*/(I^*+S^*)$] rises with f; Figure S4). However,
the R_0 criterion produced by this model remains transparent enough:

$$R_0 = \left(\frac{f}{m}\right)(\sigma u - 1)S_{\mathrm{bnd}}^* \tag{B3}$$

where S_{bnd}^* is was given already (equ. 3). Here, R_0 increases with contact/removal rate of spores
(f) and per-spore infectivity of the parasite (u) (with a minimal requirement that $\sigma u > 1$). Notice
that, like in the simpler version (equ. 2), birth rate of infected hosts (ρ) does not enter this
expression. Using the partial derivative approach again, we can study how this R_0 expression
changes with resource quality, Q (by deriving a similar expression as equs 4 and B1):

$$\frac{\partial R_0}{\partial Q} = R_0\left[\frac{\sigma u}{\sigma u - 1}\left(\frac{\partial \sigma}{\sigma \partial Q} + \frac{\partial u}{u \partial Q}\right) + \frac{\partial f}{f \partial Q} + \left(\frac{d}{b - d}\right)\left(\frac{\partial b}{b \partial Q}\right)\right] \tag{B4}$$

where here we are assuming that per-host spore production (σ), per –spore infectivity (u),
maximal birth rate of infected hosts (b), and clearance rate (f) all depend on quality. As before
we assume that b and σ increase with quality, but the dependence of clearance rate on quality
seems unclear for *Daphnia*. Previous studies indicate that filtering rate decreases with increased
quality ($\partial f / \partial Q < 0$; Plath and Boersma 2001, Darchambeau and Thys 2005) or increases
($\partial f / \partial Q < 0$; Richman and Dodson 1983 L&O, MacKay and Elser 1998, Schatz and McCauley
2007) with enhanced resource quality. Detailed studies in our study lakes suggest that feeding
rate does not change with resource quality ($\partial f / \partial Q \approx 0$; DeMott et al. in prep), which would then
suggest that enhancement of transmission with poorer quality mainly involves variation in per-
spore infectivity (u). In principle, in some situations, the effects of Q on f and u could contradict
each other. Regardless, this partial derivative shows us how R_0 can increase or decrease with

quality (Q), depending on the effects of quality on these key components of the interactions between hosts and parasites.

95

Additional references cited:

Darchambeau, F. & Thys, I. (2005). In situ filtration responses of *Daphnia galeata* to changes in food quality. *J. Plank. Res.,* 27, 227–236.

MacKay, N.A. & Elser, J.J. (1998). Factors potentially preventing trophic cascades: food

100   quality, invertebrate predation, and their interaction. *Limnol. Oceanogr.,* 40, 1209-1214.

Plath, K. & Boersma, M. (2001). Mineral limitation of zooplankton: stoichiometric constraints and optimal foraging. *Ecology*, 82, 1260–1269

Richman, S. & Dodson, S.I. (1983).   The effect of food quality on feeding and respiration by *Daphnia* and *Diaptomus*. *Limnol. Oceanogr.,* 28, 948–956.

105   Schatz, G.S. & McCauley, E. (2007). Foraging behavior by *Daphnia* in stoichiometric gradients of food quality. *Oecologia*, 153, 1021-1030.

Figure S4. Relationships between equilibrial density of susceptible (S^*) and infected (I^*) hosts, prevalence of infection ($p^* = I^*/(S^* + I^*)$), and feeding/clearance rate (f) as predicated by a model in which both host classes remove (consume) spores of a fungal parasite. Susceptible hosts decrease while prevalence increases with f; however, infected hosts first increase, then decrease with f. When feeding rate is low, density of infected hosts increase with f as more susceptible hosts contact spores. However, once susceptible host density drops and infected hosts become more prevalent, the latter essentially serve as sinks for spores, removing them from the water column and reducing contact of spores with S. Other parameters values: $b = 0.4$; $\rho = 0.5$; $c = 1/50$; $d = 0.05$; $u = 0.001$; $v = 0.1$; $\sigma = 50{,}000$; $m = 0.1$.
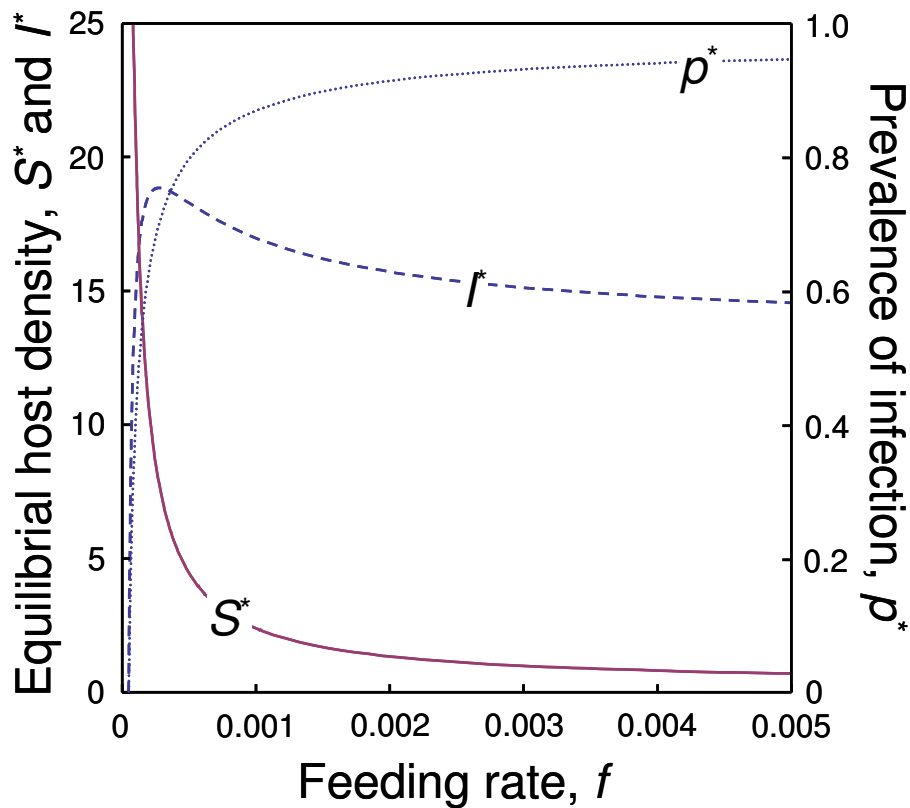
Supplemental Appendix S3: Moving from the experiments to the R_0 calculations

120

  In this Appendix we detail how we used the life table and transmission rate assays to parameterize our calculations of the reproductive ratio, R_0, for fungal epidemics in *Daphnia* populations. To relate maximal instantaneous birth rate (*b*) of uninfected hosts with the juvenile growth rate index of quality, we calculated the instantaneous rate of increase (*r*), using the life

125 table data (assuming that $b = r$; Figure 2d). Using these data, we calculated age specific survivorship, l_x, and age specific mean fecundity, m_x, at day x for each resource quality source; using calculations, we estimated r by iteratively solving the Euler equation:

$$1 = \sum l_x m_x \exp(-rx). \tag{C1}$$

Based on these calculations, we see that instantaneous birth rate relates strongly to mean

130 fecundity rate (*F*, Figure 2D) following a regression between *b* and $\ln(F)$ (Figure S5a). Still, we find a strong relationship between resource quality (indexed by juvenile growth rate, *g*) and *b* (Figure S5b). However, we should acknowledge a bias in the data: instantaneous birth rates at poor food conditions in the life table almost certain are too high because animals started the life table in energetically good conditions (and had more babies initially than they would if they had

135 been raised on poor food since birth). Regardless of this bias, in the absence of the temperature (*T*) correlation (Figure S3), we assume a linear relationship between instantaneous birth rate and quality. However, assuming that *b* also declines with temperature following the Arrhenius model (equ. 5, assuming $\gamma = 1$), we find that birth rate increases much more moderately with resource quality (Figure S5.c). This assumption closely resembles the pattern that we

140 documented in the lakes (i.e., variable birth rate with surprisingly little upward trend despite large increases in resource quality; Figure S2).

  We moved from proportion infected to transmission rate by fitting a simple differential equation model. First, we used infection data from 25 and 75 spores per mL treatments (Figure S5d). Then, we integrated the system of differential equations over a day of exposure:

145   $dS/dt = -\beta SZ$ (C2.a)

$$dI/dt = \beta SZ \tag{C2.b}$$

where susceptible (i.e., uninfected) hosts (S) became infected hosts (I) after contacting spores (Z) with per capita transmission rate β. To find the best maximum likelihood estimates (MLE) of the parameter β, we assumed that error in prevalence of infection was distributed binomially. The

150   binomial error distribution applies to situations in which only two outcomes (i.e., infected or not-infected) occur in trials repeated N times (where N is the number of hosts in each beaker). If p is the predicted prevalence (probability) of infection of a host (from equ. C2), then I hosts become infected among all N hosts within a beaker with probability (Hilborn and Mangel 1997:64):

$$p(I,N) = \binom{N}{I} p^I (1-p)^{N-I}. \tag{C3}$$

155   When infection prevalence p is calculated by integrating the skeleton model (equ. C2), this binomial distribution (equ. C3) provides the likelihood of the outcome observed in each beaker, given the data and prevalence predicted by the parameters. Over the entire experiment, one can then sum the negative log-likelihood of the results from each beaker; the MLE of the parameter (β) minimizes the summed negative log likelihood of the experiment (Hilborn and Mangel 1997).

160   These MLE parameters were located using a standard search algorithm (Nelder-Mead downhill simplex) as implemented by Matlab 5.3 (Mathworks, Inc. 1999). We fit both linear and exponential models through the growth rate-transmission rate estimates; based on AIC values calculated for both models (Burnham and Anderson 2002), we concluded that the exponential model fit best – transmission rate declined exponentially with resource quality (Figure S5e).

165   Using this parameterized model for the R_0 calculations (Figure 4), we see that transmission rate (β) declines with increasing resource quality (g). Once the growth rate-temperature (T) correlation (Figure S3) is added following the Arrhenius function (equ. 5, $\gamma = 3$), transmission rate declines even more rapidly with quality (Figure S5f). This joint resource quality-temperature effect on transmission is the figurative "double whammy" to which we refer in the

170   text.

Literature Cited

Burnham, K.P. & Anderson, D.R. (2002). *Model selection and multimodel inference: a practical information-theoretic approach*. Springer, New York, NY USA.

175   Hilborn, R. & Mangel, M. (1997). *The ecological detective: confronting models with data*. Princeton University Press, Princeton, NJ, USA.

MathWorks, Inc. (1999). *Matlab 5.3: the language of technical computing*. The MathWorks, Inc., Natick, MA.

Figure S5. Further work to show how reproductive ratio (R_0) changes with resource quality (g)

180   and temperature (T) as shown in Figure 4 of the text. (A)-(C) involve calculation of

instantaneous birth rate, b. (A) After calculating b from the life table data using the Euler

equation (equ. C1), we find a very strong relationship between the natural log of average birth

rate (F; Figure 2d) and b. (B) These estimates of b still relate quite linearly to the growth rate

index of resource quality. (C) We illustrate how we use this regression to show how b changes

185   with g, ignoring the resource quality (g)-temperature (T) correlation that we see in the field (i.e.,

the $b(g)$ curve). Then, we include the joint effects of g and T on b (i.e., the $b(g, T)$ curve –

cooling temperatures remarkably moderate the positive effects of resource quality on birth rate.

Panels (D)-(F) involve calculation of transmission rate (β). (D) We calculated it from data on

proportion infection using the 25 spore/mL treatment (Figure 3) and the 75 spore/mL treatment.

190   (E) Using the estimates of transmission rate, we found a linear relationship between $\ln(\beta)$ and the

growth rate index of quality (g). (F) With that equation, we then see that transmission rate

declines with quality, particularly if we include the quality-temperature (T) correlation. In panels

(C) and (F), we show both resource quality and temperature as two X-axes.

195